IAC-11-A2.5.9

RE-ENTRY ANALYSIS OF RESEARCH ROCKET PAYLOADS

Andreas Stamminger
Deutsches Zentrum für Luft- und Raumfahrt (DLR), *Mobile Rocket Base, Oberpfaffenhofen, 82234 Wessling*, Germany, Tel.: +49-*8153-28-1231*, Email: andreas.stamminger@dlr.de

The atmospheric re-entry of sounding rocket payloads is an important phase of ballistic flight, especially if instruments and experiments are to be recovered for future flights or interpretation of experimental data. Understanding the dynamic behaviour of cylindrical and cone-cylindrical payloads during the re-entry is a prerequisite for ensuring successful deployment of the parachute system[1 2]. This includes not only knowledge of the payload vehicle attitude and rate data but also the "global view" of deceleration, descent time and terminal recovery velocity. The paper describes the analysis work that has been conducted at the German Aerospace Center's Mobile Rocket Base on the flight data of several TEXUS (Technologische EXperimente Unter Schwerelosigkeit) and MAXUS payloads that have been reviewed and compared. Vehicles, in which the centre of gravity coincides with the longitudinal aerodynamic centre, as is the case with TEXUS, MAXUS and MASER payloads, are usually spun-up about the longitudinal axis before entry into the atmosphere to eliminate concentration of surface aerodynamic heating and enhance the condition for a flat-spin. Analyses of flight data have shown that the payload spinning stops when dynamic pressure starts to build and it is stabilised to one lateral position depending on devices like Telecommando- or GPS-Antennae before the payload reaches the flight time with maximum deceleration. The differences in the flow separation, forces the cylindrical payload into a rotational motion about the axis of highest inertial moment when it reaches subsonic velocity. During the analysis work that has been conducted at the Mobile Rocket Base, flight data from several TEXUS and MAXUS payloads have been reviewed and compared. The availability of accurate GPS and sensor data support the analysis of the acceleration of the payload from a altitude of 120 km during descent. With the use of gravitation models the acceleration is reduced to its aerodynamic component only. The density of the atmosphere is taken from atmospheric models to calculate the drag coefficient which is dependent on payload attitude, Reynolds-Number and Mach-Number. Up to now estimations for drag coefficients have been based on theoretical data and measurements of a cylinder in a flow field of a certain Reynolds-Number. Modelling the re-entry has also been performed by simulating the payload motion during its flight through the atmosphere, as well as the change of the drag. This paper describes the similar behaviour of the drag coefficient for sounding rocket payloads regarding the dependence on geometry, Reynolds-Number and Mach-Number.

I. INTRODUCTION

Numerous Sounding Rockets have been launched and the behaviour of the payloads has been investigated in studies. Nevertheless some missions that had non-successful recoveries or a loss of telemetry-data during re-entry showed that an improved analysis of the behaviour of the payload during this phase of the flight is necessary. As an example the SHEFEX-1 and CUMA-2 mission should be mentioned.

The importance of analysis of risk to populations by the re-entry of ballistic vehicles as well as of objects that return from orbit to Earth has increased in recent years. Many tools have been developed to investigate trajectories and the destruction progress of space vehicles and rocket assemblies during re-entry[3]. It is assumed that the space vehicle breaks apart at altitudes between 85 and 75 km and the impact point of each peace of debris can be calculated because position and velocity vector are known. Similar to the analysis presented in this paper the ballistic coefficient has to be known. Therefore it is nearly impossible to simulate the re-entry of a complex structure like a complete space station including the heating of each module. For analysis of the sounding rocket payloads a simpler method without aerothermodynamic calculations has been used. This simpler method has also been used in the flight safety of satellite launchers for the assumption of worst-case scenarios. In this model it is assumed that the rocket stage enters the atmosphere stable and aligned longitudinally or perpendicularly to the flight direction to calculate the re-entry trajectory[4].

CUMA-2 Payload Re-Entry

One example that shows the necessity of good knowledge of the behaviour of a payload during re-entry is the error analysis of the CUMA-2 flight. CUMA-2 was launched on the 19th July 2007 on a VSB-30 rocket in Alcântara, Brazil. The telemetry station had problems tracking the payload during flight and lost contact with the payload at apogee. A backup station in Natal, 1000

km away, received the telemetry data including GPS position data until 464 s after lift-off[5] [6]. Because of the Earth's curvature the payload can only be tracked to an altitude of 57 km before the signal is lost. The next figure shows the CUMA-2 re-entry configuration.

Fig. 1: CUMA-2 Payload Re-Entry Configuration

The station in Alcântara receives data again 505 s after lift-off but the GPS receiver cannot calculate any position solutions for the payload. The flight altitude can be determined using the slant-range data of the telemetry station. Due to the low elevation at this flight time this calculation has only a low accuracy. The video pictures show that the payload is aligned horizontally and the incoming air flow is perpendicular to the payload's longitudinal axis. Clouds can be observed over the sea on the video pictures but it is impossible to estimate the altitude without reference. The telemetry reception finally stops after the payload disappears over the horizon. The helicopter recovery of the payload in the sea was not successful because the payload was not detected. The important 40 s during the hard re-entry when the payload is decelerated from super sonic to sub sonic velocity are missing for a failure analysis. Question that remain unanswered are: Why did the GPS receiver not deliver any GPS position solutions? At which altitude were the received video pictures recorded and should the activation of the parachute recovery sequence be visible on the video pictures? What accelerations appeared during re-entry? Did the accelerations lead to a premature activation of the parachute deployment? To answer these questions the results of the analysis of flown payloads presented in this paper have been used to reconstruct the missing re-entry trajectory of CUMA-2.

II. PAYLOAD RE-ENTRY CONFIGURATIONS

Sounding rocket payloads are usually cylindrical or cone-cylindrical bodies containing modules for experiments, all necessary service systems and recovery. During re-entry all considered payloads have a cylindrical shape, because the nose cone is separated after burn-out of the last stage. The payloads differ in diameter D_{PL}, 0.438 m for TEXUS and 0.64 m for MAXUS, but the ratio of length L_{PL} to diameter D_{PL} is comparable. The following figure shows some of the analyzed payloads.

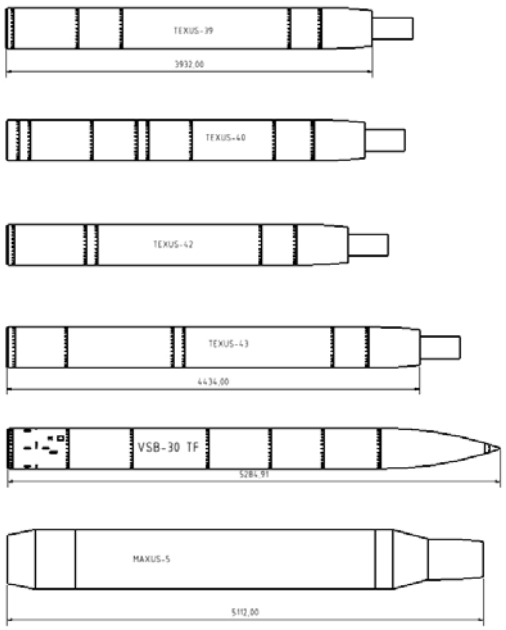

Fig. 2: Payload Re-Entry Configuration of TEXUS-39, 40, 42, 43, VSB-30 TF and MAXUS-5.

The payload ratio length to diameter varies between $\frac{L_{PL}}{D_{PL}} = 7.88$ (MAXUS-7) to $\frac{L_{PL}}{D_{PL}} = 10.12$ (TEXUS-43). The TEXUS payloads in figure 2 are shown with the nose cone ejection can that is connected with the heat shield until the aerodynamic loads increase during re-entry and it bursts off.

The considered TEXUS payload re-entry mass m_{PL} varies between 361 kg[7] to 397 kg[8]. The MAXUS payloads re-entry mass m_{PL} differs from 704 kg to 729 kg[9].

To avoid a stable re-entry, the centres of gravity of these payloads coincide with the longitudinal aerodynamic centres. As an example, the following figure shows the TEXUS-43 payload.

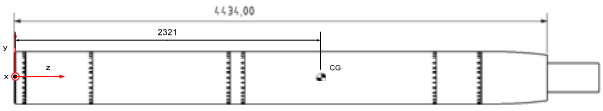

Fig. 3: TEXUS-43 Re-Entry Configuration with Nose Cone Ejection Can.

Referenced to the payload length L_{PL} the TEXUS-43 centre of gravity is placed 52 % from the separation plane. The distance between centre of gravity $z_{BF,cg}$ and aerodynamic centre $z_{BF,cp}$ referenced to the payload length L_{PL} is around 2 % which is more distant than for TEXUS payloads that have been launched before.

III. FLIGHT DATA ANALYSIS

The next figure shows the schematic approach of the analysis of the payloads during re-entry with measured flight data.

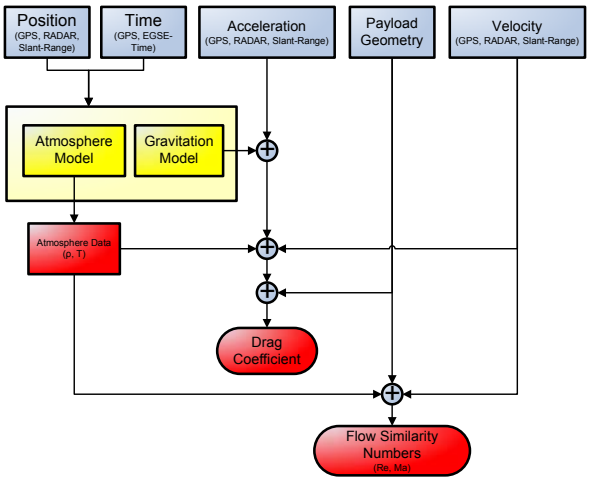

Fig. 4: Schematic diagram of the calculation of the drag coefficient of the payload and the similarity parameters

The flight parameter position $\vec{r}$ is preferably taken from GPS data. If no GPS-Data is available the position is determined from RADAR or slant range data. The velocity $\dot{\vec{r}}$ and acceleration $\ddot{\vec{r}}$ of the payload in respect to the Earth are determined by differentiation of the positional data with respect to time. In a high dynamic flight phase, such as atmospheric re-entry, the use of GPS leads to far more accurate results. Nevertheless the position of the GPS antennas should be well known to avoid a misinterpretation of the movement of the payload when the payload has a fast rotation movement like a flat spin. The next schematic diagram shows the calculation of the flight parameter from positional data. An explanation of the coordinate systems and the transformation matrix can be found in a thesis conducted at DLR[10].

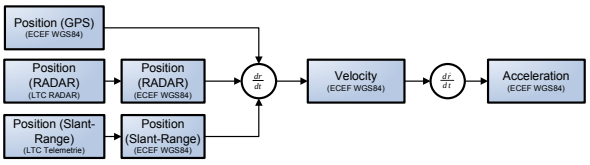

Fig. 5: Determination of the Flight Parameters with GPS, RADAR and Slant Range Data

The GPS receiver delivers the velocity directly in the VCVF coordinate system.

Fig. 6: Calculation of the Acceleration Data with GPS Data

In order to calculate the influence of the atmospheric drag on the observed movement of the payload it is necessary to know the gravitational acceleration of the Earth.

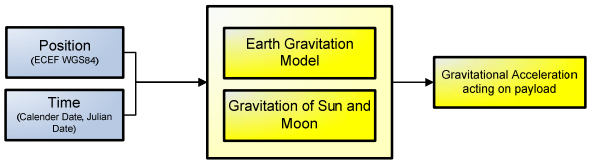

Fig. 7: Calculation of the gravitational acceleration that acts on the sounding rocket payload

The atmospheric models used need the position of the payload as input. The CIRA86 and Harris-Prister-Model are also time dependent. The models are necessary to calculate the density and temperature at the position of the payload during re-entry.

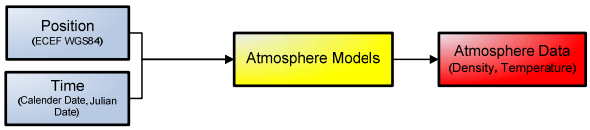

Fig. 8: Calculation of atmospheric data

IV. TYPICAL RE-ENTRY OF A SOUNDING ROCKET PAYLOAD

Vehicles, in which the centre of gravity coincides with the longitudinal aerodynamic centre, as is the case with TEXUS, MAXUS and MASER payloads, are usually spun-up about the longitudinal axis before re-entry into the atmosphere to eliminate concentration of surface aerodynamic heating and enhance the condition for flat spin[11]. Analysis of flight data has shown that the payload spinning stops when dynamic pressure starts to build and it is stabilized to one lateral position depending on protuberances like telecommand- or S-band-antennae, before the payload reaches the flight time with maximum deceleration.

E.g. in figure 9, the MAXUS-6 has been spun up at an altitude $h_{ECEF} \approx 72$ km to a maximum spin rate $\dot{p} \approx 300 \frac{^\circ}{s}$ but the roll motion stops at an altitude of 30 km after nearly 12 seconds. At this flight time the payload has reached one third of its maximum deceleration peak $a_{BF} \approx 41$ g .

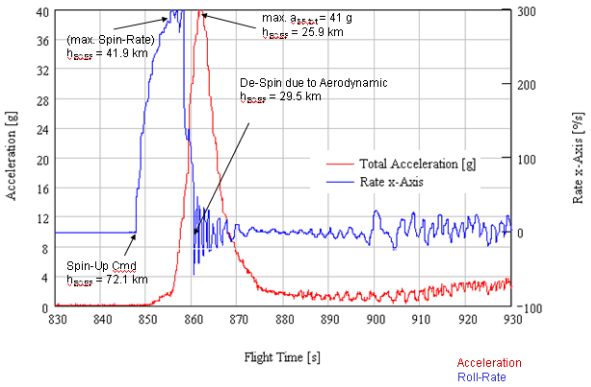

Fig. 9: MAXUS-6 – Acceleration $a_{BF,tot}$ (Accelerometer, red) and Roll-Rate $\dot{p}$ (Rate-Sensor, blue) during the re-entry[12]: The spin rate is stopped before the maximum acceleration

If acceleration data from GPS and the lateral accelerometers are compared, conclusions on the attitude of the payload are possible. If both curves coincide, the payload has an attitude that is perpendicular to the incoming flow. This applies to the re-entry behaviour of the MAXUS-6 payload (see figure 9), also the difference in acceleration data at higher altitudes indicates that the payload enters the higher atmosphere with the re-entry cone slightly ahead.

If the body-fixed acceleration data is not disturbed by roll rotation or flat spin motion, it is also possible to calculate a pseudo angle of attack σ. For a very stable period with a pseudo angle of attack $\sigma = -1°$ this is shown for the MAXUS-7 payload in the next figure.

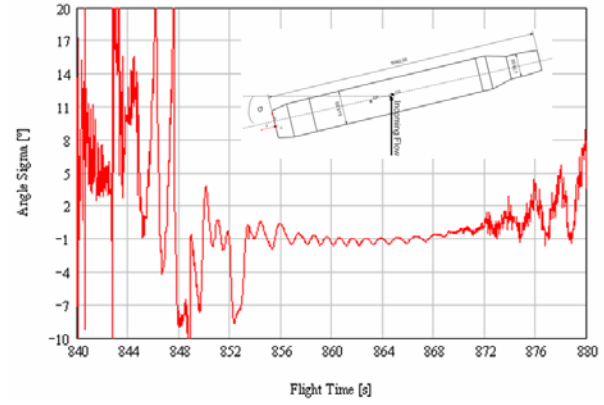

Fig. 10: MAXUS-7 – Angle σ during Re-entry till Beginning of the Flat Spin

As already mentioned payloads stop the roll motion with the increase of aerodynamic loads and stabilize to a lateral position between the telecommand-antennae. TEXUS-43 adopts a position $Pos_{AeroFlow} \approx 322°$ referring to the cross section in figure 11. In addition, this incoming flow is indicated by the temperature sensors on the payload structure[13]. The MAXUS-7 payload is also stabilized between the telecommand-antennae and traces of ablation can be found also on the recovered payload structure at the position that is indicated by the acceleration data.

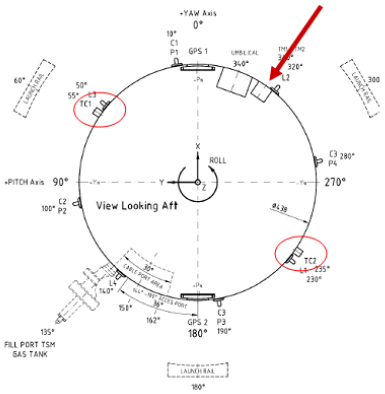

$Pos_{AeroFlow} \approx 322°$

Fig.11: TEXUS-43 – Lateral Flow Position

The flat spin occurs during the sub sonic flight after crossing the critical Reynolds number Re = 300000. Asymmetries and protuberances cause a turbulent flow regime behind the separation of the laminar flow on one side of the payload.

.

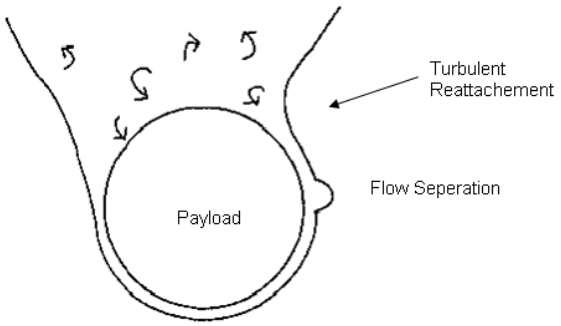

Fig.12: Asymmetric Flow Field around a cylinder at Critical Reynolds-number

The differences in the flow separation force the cylindrical payload into a rotational motion about the axis of highest inertial moment when it reaches subsonic velocity. The flat spin rate of the MAXUS-7 payload is shown in the next figure.

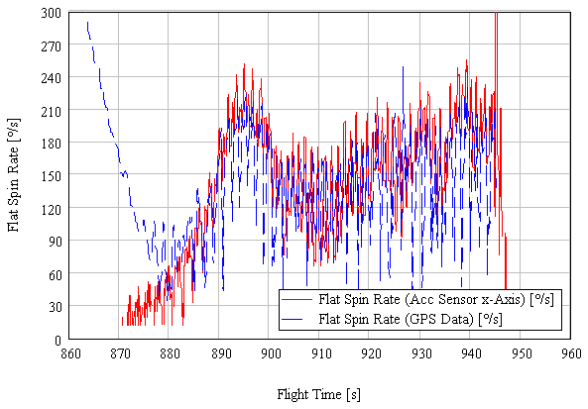

Fig.13: Flat Spin Rate, calculated with GPS and Accelerometer Data

If the payload does not change the velocity in a horizontal direction and a perpendicular attitude to the flight vector is assumed, it is possible to calculate the flat spin also with GPS acceleration data. The payload passes the supercritical Reynolds-Numbers twice during re-entry.

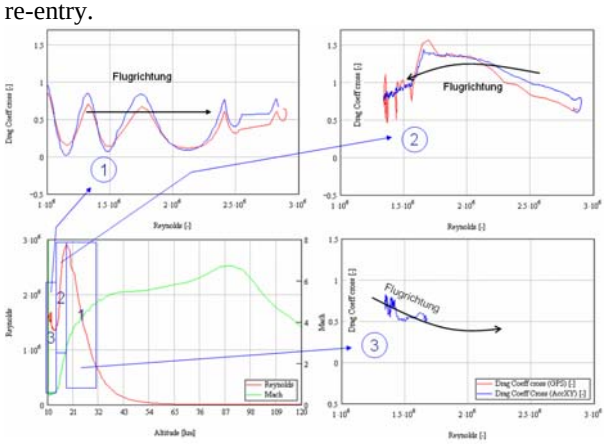

Fig.14: TEXUS-43 – Drag Coefficient $c_{D,\square}$ vs. Reynolds-Number in Supercritical Flow Regime[14]

V. DRAG COEFFICIENT MODEL

There two ways are possible ways to simulate the trajectory of a payload during re-entry. The first approach is to calculate the dynamic behaviour of the payload from the beginning of the re-entry at an altitude of 120 km until the activation of the recovery sequence regarding aerodynamic forces, moments and damping moments.

The attitude movement of the payload can only be calculated with uncertainties. The attitude of the payload is used in this method to estimate the drag coefficient that is also dependent on Reynolds- and Mach-Number.

The solution that is presented in this paper is a simpler approach. Regarding the typical behaviour of a payload during re-entry, as described in the preceding chapter, it is also possible to estimate this behaviour also for similar payloads. With these boundary conditions it is possible to normalize the payload and define a mean drag coefficient $c_{D,\square}(h_{ECEF})$ dependent on the altitude. It is necessary to use different diagrams for TEXUS and MAXUS because of the different re-entry velocities, as well as apogees of both missions.

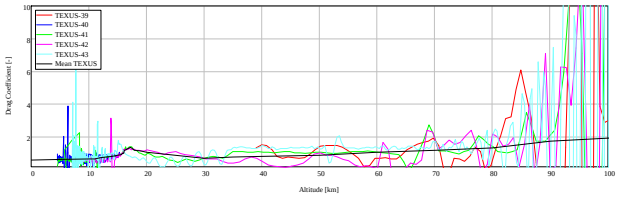

Fig.15: Drag Coefficient $c_{D,\square,TEXUS}(h_{ECEF})$ dependent on the geodetic altitude h_{ECEF} for TEXUS payloads

Validation

A validation of the data is done by comparison of real flight data and the calculated values by simulating the re-entry of the same payload with known position and velocity at 120 km altitude. The following figure shows the comparison between real acceleration of the MAXUS-6 payload and simulated data using the drag coefficient $c_{D,\square,MAXUS}(h_{ECEF})$.

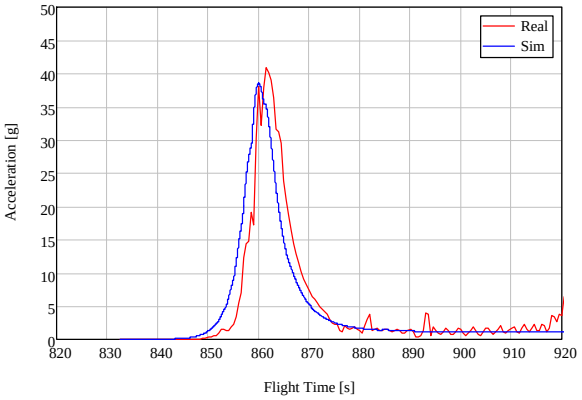

Fig.16: MAXUS-6 – Comparison of real acceleration data a_{BF} and simulated acceleration data using the drag coefficient $c_{D,\square,MAXUS}(h_{ECEF})$

Reconstruction of CUMA-2 Flight Data

This simulation method can also be used for the reconstruction of lost flight data. The loss of the telemetry signal in the CUMA-2 mission has been

mentioned in the introduction. The next table shows the reconstructed flight data of CUMA-2.

Time Event	Altitude h_{ECEF} [km]	Flight Time t [s]
Lift-Off	0.1	0.0
Ignition of Spin-Up Motors	0.1	0.4
Max. Acceleration $a_{BF} = 7.8$ g	0.2	2.4
Burn-Out 1st Stage	3.0	11.2
Booster Separation	-	-
Ignition 2nd Stage	4.9	15.2
Max. Acceleration $a_{BF} = 11.7$ g	24.6	35.0
Max. Velocity $v_{VCVF} = 2045.3 \frac{m}{s}$	36.4	41.2
Burn-Out 2nd Stage	41.6	43.7
Nose Cone Ejection	61.8	54.4
Yo-yo De-spin	65.1	56.1
Motor Separation	70.6	59.1
RCS Activation	75.7	62.0
Start of Microgravity (>100 km)	100.0	76.0
Apogee	249.5	257.8
End of Microgravity (<100 km)	100.0	440.2
Max. Mach-Number during re-entry $Ma = 6.49$	74.8	454.8
Last GPS Position	56.9	464.6
Begin of Spin-Up	(Sim) 56.1	465.0
Max. Dynamic Pressure ($q_{max} = 27.7$ kPa)	(Sim) 26.6	(Sim) 482.3
Max. Deceleration ($a_{BF} = 13.5$ g **(Sim)**)	(Sim) 25.8	(Sim) 483.0
1. Max Reynolds-Number ($Re = 1.82 \cdot 10^6$)	(Sim) 21.9	(Sim) 486.8
20 km during descent	20.0	(Sim) 489.9
Mach 1	(Sim) 17.5	(Sim) 496.3
Begin of telemetry data received from Alcântara	(Sim) 15.6	505.0
Loss of telemetry data from Alcântara	(Sim) 5.9	584.0
Heatshield (Terminal Vel. $v_{VCVF} = 82 \frac{m}{s}$ **(Sim))**	(Sim) 4.6	(Sim) 598.3
Stab Chute De-reefed	(Sim) 4.1	(Sim) 607.5
Main Chute	(Sim) 3.5	(Sim) 620.9
Main Chute De-reefed	(Sim) 3.2	(Sim) 634.0
Landing	(Sim) 0.1	~1000.0

Table 1: Flight Events CUMA-2 (GPS, Simulation)

This leads to the result that the Alcântara station receives payload data at an altitude of 16 km and contact is finally lost at an altitude of 6 km before the nominal altitude of the activation of the recovery sequence. A deployment of the parachute should not be visible on the video pictures.

VI. SUMMARY & OUTLOOK

The analysis presented in this paper has focused on the similar behaviour of sounding rocket payloads during re-entry. The drag coefficient dependence on geometry and Reynolds- and Mach-Number has been shown with real flight data.

This data is not only interesting for a post-analysis of a sounding rocket flight but also for re-entry simulation of future flights. The data that is presented in this paper has been used to build an empirical model that calculates drag coefficient only dependent on payload geometry and altitude. Flown payloads have been simulated and the trajectories and interesting events during re-entry have been validated with real flight data. A use of this simple model has been shown on the CUMA-2 example.

The work presented in this paper can be used to improve future trajectory predictions especially when the time of the flight events is a critical issue. For the future it would be interesting to analyze the behaviour of smaller payloads as used in REXUS and MAPHEUS missions.

[1] Tong, Donald:, *Payload Vehicle Aerodynamics Re-Entry Analysis*, Journal of Spacecraft And Rockets, Vol.29, No. 5, 1992

[2] Krause, David: *NSROC, Recovery Systems and Mesquito Vehicle Developments*, 18th ESA Symposium on European Rocket and Balloon Programmes and Related Research, Visby, Sweden, 2007

[3] Lips, Tobias / Fritsche, Bent: *A comparison of commonly used re-entry analysis tools*, HTG Hypersonic Technology Göttingen, 2005

[4] Sentenai, Alina: *Aerodynamic and Thermal Analysis of the Soyuz Launcher in Kourou, French Guiana*, TU München, RT-DA 05/03, 2005

[5] Stamminger, Andreas, 2007, *CUMA-2 Re-Entry Analysis*, Deutsches Zentrum für Luft- und Raumfahrt, RB-MR

[6] Ettl, Josef: *CUMA-2 Technical Report*, Deutsches Zentrum für Luft- und Raumfahrt, 2008

[7] Jung, Wolfgang: *TEXUS EML-1Pre-Launch Report*, Deutsches Zentrum für Luft- und Raumfahrt, RB-MR 2005

[8] Jung W. / de Magalhães Gomes R.: *TEXUS-43 Pre-Flight Report*, Deutsches Zentrum für Luft- und Raumfahrt, RB-MR, 2006

[9] Astrium: *MAXUS-4 Flight Preperation and Mission Performance Report*, Astrium GmbH, 2001

[10] Stamminger, Andreas: *Beiträge zum Verhalten von Raketennutzlastkörpern beim atmosphärischen Wiedereintritt*, TU München, 2011

[11] Tong, D.: *Payload Vehicle Aerodynamics Re-Entry Analysis*, T Journal Of Spacecraft And Rockets, Vol. 29, No.5, September-October 1992

[12] Stamminger, Andreas: *MAXUS-5 Re-Entry Analysis*, Deutsches Zentrum für Luft- und Raumfahrt, RB-MR, 2007

[13] Pfeuffer, Horst: *TEXUS-43 Post Flight Review*, Kayser-Threde GmbH, 2006

[14] Stamminger, Andreas, 2007, *Atmospheric R-Entry Analysis of Sounding Rocket Payloads*, 18th ESA Symposium on European Rocket and Balloon Programmes and Related Research, Visby, Sweden